ISSN 1070-3284, Russian Journal of Coordination Chemistry, 2024, Vol. 50, No. 4, pp. 269–280. © Pleiades Publishing, Ltd., 2024.

Coordination Compounds of Cobalt(II) Nitrate and Perchlorate with Acetamide and Carbamide: Precursors for the Synthesis of Catalytically Active Tricobalt Tetraoxide

R. A. Rodriguez Pineda[a], *, I. A. Karavaev[a], E. V. Savinkina[a], E. V. Volchkova[a], Zh. Yu. Pastukhova[a], L. G. Bruk[a], G. A. Buzanov[b], A. S. Kubasov[b], and V. M. Retivov[c]

[a] *Lomonosov Institute of Fine Chemical Technologies, MIREA Russian Technological University, Moscow, Russia*

[b] *Kurnakov Institute of General and Inorganic Chemistry, Russian Academy of Sciences, Moscow, Russia*

[c] *National Research Center Kurchatov Institute, Moscow, Russia*

**e-mail: rodrigues.pineda@yandex.ru*

Received October 15, 2023; revised December 10, 2023; accepted January 10, 2024

Abstract—The reactions of cobalt(II) nitrate or perchlorate with acetamide (AA) or carbamide (Ur) in an aqueous medium results in formation of coordination compounds $[Co(Ur)_4](NO_3)_2$ (**I**), $[Co(Ur)_6](NO_3)_2$ (**II**), $[Co(AA)_4(H_2O)_2](NO_3)_2$ (**III**), $[Co(AA)_4(H_2O)_2](NO_3)_2 \cdot 2AA$ (**IV**), $[Co(Ur)_6](ClO_4)_2$, (**V**), $[Co(AA)_4(H_2O)_2](ClO_4)_2$ (**VI**), and $[Co(AA)_6](ClO_4)_2$ (**VII**). The compositions of the isolated complexes are determined by physicochemical methods, and the crystal and molecular structures of compounds **II**, **V**, **VI**, and **VII** are solved. Specific features of the thermal behavior of all synthesized compounds in a wide temperature range are studied in detail. These compounds are shown to be used as precursors in the preparation of nanosized Co_3O_4 using self-propagating high-temperature synthesis. The catalytic activity of thus synthesized Co_3O_4 in the model epoxidation of allyl alcohol is studied.

Keywords: cobalt(II) nitrate, Cobalt(II) perchlorate, acetamide, carbamide, self-propagating high-temperature synthesis, nanosized tricobalt tetraoxide

DOI: 10.1134/S1070328424600049

INTRODUCTION

Self-propagating high-temperature synthesis, including its modification known as "solution combustion synthesis" (SCS), is a promising method for the preparation of nanosized transition element oxides [1, 2]. This method uses systems containing simultaneously (along with ions of the necessary metal) both component-oxidants (as a rule, nitrate ions) and component-reducing agents (fuel), the role of which is played, for example, by glycine (Gly) [3], citric acid [4], dimethylformamide [5], carbamide (Ur) [6], and other organic compounds. Coordination compounds can be formed as intermediates in these reactions [7]. The exothermic redox reaction is initiated by heating.

Among transition metal oxides tricobalt tetraoxide is especially significant for the development of the modern technologies due to an important set of physicochemical properties [8] and, hence, it finds wide use in the preparation and processing of materials of lithium-ion batteries [9, 10], supercapacitors [11], and sensors [12], as well as a catalyst for hydrogen evolution in hydrogen energetics [13].

The preparation of Co_3O_4 by the SCS method using cobalt(II) nitrate as the oxidant and carbamide and glycine as the fuel was studied [14]. A transparent viscous gel was shown to be formed in this system and to transform on further heating into Co_3O_4, CoO, or Co depending on the nitrate/fuel molar ratio. According to the data of scanning electron microscopy, thus prepared Co_3O_4 particles are 22–105 nm in size. The compounds formed at the initial stage of interaction of the components of a $Co(NO_3)_2$–Ur/Gly–H_2O system were not studied in this work. The preparation of catalytically active Co_3O_4 by the SCS method using cobalt nitrate and glycine was described [15].

In addition to carbamide, acetamide (AA) can act as a promising fuel in the SCS method.

No published data on the preparation of cobalt oxides using cobalt(II) perchlorate as the oxidant and no structural studies of the compounds formed due to the reactions of cobalt(II) perchlorate with carbamide or acetamide are available. Of the related systems, the use of nickel(II) perchlorate and carbamide for the preparation of the NiO phase was presented [16]. Some coordination compounds of cobalt(II) nitrate with carbamide and acetamide have been studied previously, but their thermal decomposition was not studied.

The crystal structures of the coordination compounds of cobalt(II) nitrate with carbamide in molar ratios of 1 : 2, 1 : 4, and 1 : 10 were described. The Ur ligand exhibits the monodentate coordination via the oxygen atom in the structures of the $[Co(Ur)_2(H_2O)_4](NO_3)_2$ ($P\bar{1}$) [17], $[Co(Ur)_4(H_2O)_2](NO_3)_2$ ($P2_1/n$) [18], and $[Co(Ur)_6](NO_3)_2{\cdot}4Ur$ ($P\bar{1}$) [19] complexes. The *R* factors equal to 14.9 and 16.8% were determined for $[Co(Ur)_2(H_2O)_4](NO_3)_2$ and $[Co(Ur)_6](NO_3)_2{\cdot}4Ur$, respectively, which casts doubt on the accuracy of the structural parameters determination. The synthesis and results of studying the crystal and molecular structures of the coordination polymer $[Co(Ur)_4]_n(NO_3)_{2n}$ ($P2_1/c$) were presented [20, 21]. Carbamide in the synthesized compound was shown to behave as both the monodentate and bridging ligand demonstrating coordination via the donor oxygen and nitrogen atoms.

The compounds with the cobalt to acetamide molar ratio equal to 1 : 4 and 1 : 6 were synthesized in the case of acetamide. It is shown for the $[Co(AA)_4(H_2O)_2](NO_3)_2$ ($P2_1/c$) and $[Co(AA)_6](NO_3)_2$ (P-3) complexes that both the acetamide and carbamide molecules coordinate via the donor oxygen atom [22].

The purpose of this work is to optimize conditions for the synthesis and isolation of the coordination compounds of cobalt(II) nitrate or perchlorate with carbamide or acetamide, to determine the crystal and molecular structures of new compounds, to study the thermal behavior of the isolated compounds in a wide temperature range, and to examine the catalytic activity of the final product of thermolysis of the synthesized compounds.

EXPERIMENTAL

The initial substances for the synthesis of the coordination compounds were cobalt(II) perchlorate hexahydrate prepared by the reaction of basic cobalt carbonate $CoCO_3{\cdot}mCo(OH)_2{\cdot}nH_2O$ (>98%, MERCK) and per chloric acid (REAKHIM, 70% aqueous solution) followed by concentrating the solution to form crystals, cobalt(II) nitrate hexahydrate (99.9% MERCK) preliminarily recrystallized from ethanol, acetamide (99%, MERCK), and carbamide (99.9%, ABCR).

The complexes $[Co(Ur)_4](NO_3)_2$ (**I**), $[Co(Ur)_6](NO_3)_2$ (**II**), $[Co(AA)_4(H_2O)_2](NO_3)_2$ (**III**), $[Co(AA)_4(H_2O)_2](NO_3)_2{\cdot}2AA$ (**IV**), $[Co(Ur)_6](ClO_4)_2$ (**V**), $[Co(AA)_4(H_2O)_2](ClO_4)_2$ (**VI**), and $[Co(AA)_6](ClO_4)_2$ (**VII**) were synthesized by mixing stoichiometric amounts of cobalt(II) nitrate or perchlorate hexahydrates and carbamide or acetamide in an aqueous medium. Details of the synthesis are given in Supplementary Information (Table S1).

Analysis to metal was conducted by complexonometric titration. A standard solution of Trilon B served as the titrant, and murexide was used as the indicator. Titration was carried out in an ammonia buffer (pH 8–9). Analyses to C, H, and N were conducted on a CHNS Flash EA 1112 instrument.

The IR spectroscopic studies of the coordination compounds were carried out on an FSM 2201 FT-IR spectrometer (OOO Infraspek, Russia) in a range of 4000–420 cm^{-1}. Samples for detection were prepared by pressing in KBr pellets. The measurement error of absorption maxima frequencies did not exceed 3–4 cm^{-1}.

The results of chemical analysis and IR spectroscopy are as follows.

$[Co(Ur)_4](NO_3)_2$ (I)

For $CoC_4H_{16}N_{10}O_{10}$

Anal. calcd., %	C, 11.35	H, 3.78	N, 33.10	Co, 13.93
Found, %	C, 10.92	H, 4.05	N, 33.94	Co, 12.82

IR (ν, cm^{-1}): 3449 s, 3366 s, 2402 w, 1640 s, 1475 m, 1384 s, 1159 m, 1019 w, 935 w, 826 m, 778 w, 598 m, 534 m.

$[Co(Ur)_6](NO_3)_2$ (II)

For $CoC_6H_{24}N_{14}O_{12}$

Anal. calcd., %	C, 13.26	H, 4.42	N, 36.10	Co, 10.85
Found, %	C, 13.20	H, 4.45	N, 37.13	Co, 10.61

IR (ν, cm^{-1}): 3449 s, 3366 s, 2362 w, 2334 w, 1644 s, 1475 m, 1384 s, 1159 m, 1015 w, 826 w, 778 w, 606 m, 534 m.

$[Co(AA)_4(H_2O)_2](NO_3)_2$ (III)

For $CoC_8H_{24}N_6O_{12}$

Anal. calcd., %	C, 21.10	H, 5.28	N, 18.47	Co, 12.95
Found, %	C, 21.14	H, 5.31	N, 18.33	Co, 12.21

IR (ν, cm^{-1}): 3372 s, 3200 s, 2791 w, 2430 w, 2398 w, 2277 w, 2117 w, 1765 m, 1660 s, 1596 s, 1460 w, 1380 s, 1135 m, 1043 m, 886 w, 826 w, 637 m, 482 m.

$[Co(AA)_4(H_2O)_2](NO_3)_2{\cdot}2AA$ (IV)

For $CoC_{12}H_{34}N_8O_{14}$

Anal. calcd., %	C, 25.14	H, 5.93	N, 19.55	Co, 10.28
Found, %	C, 26.26	H, 6.02	N, 20.36	Co, 10.77

IR (ν, cm^{-1}): 3348 s, 3200 s, 2794 m, 2438 w, 2362 w, 2290 w, 2145 w, 1664 s, 1612 m, 1460 m, 1400 s, 1386 s, 1135 m, 1038 m, 886 w, 830 w, 766 w, 698 m, 630 m, 590 m, 474 m.

$[Co(Ur)_6](ClO_4)_2$ (V)

For $CoC_6H_{24}N_{12}O_{14}Cl_2$

Anal. calcd., %	C, 11.65	H, 3.88	N, 27.19	Co, 9.53
Found, %	C, 11.80	H, 3.96	N, 27.29	Co, 8.90

IR (ν, cm^{-1}): 3468 s, 3337 s, 2803 m, 2269 m, 2480 w, 2296 w, 2179 w, 2062 w, 2020 w, 1631 s, 1577 s, 1476 s, 1150 s, 1108 s, 1087 s, 941 m, 773 m, 623 s, 531 s.

$[Co(AA)_4(H_2O)_2](ClO_4)_2$ (VI)

For $CoC_8H_{24}N_4O_{14}Cl_2$

Anal. calcd., %	C, 18.12	H, 4.53	N, 10.57	Co, 11.12
Found, %	C, 18.37	H, 4.53	N, 11.07	Co, 10.95

IR (ν, cm^{-1}): 3392 s, 2999 s, 2785 m, 2334 w, 2120 w, 2020 w, 1769 w, 1660 s, 1589 m, 1455 m, 1405 s, 1141 s, 1113 s, 1087 s, 937 w, 891 w, 853 w, 782 w, 686 m, 627 s, 585 m, 477 w.

$[Co(AA)_6](ClO_4)_2$ (VII)

For $CoC_{12}H_{30}N_6O_{14}Cl_2$

Anal. calcd., %	C, 20.53	H, 4.90	N, 13.73	Co, 9.63
Found, %	C, 20.50	H, 4.85	N, 14.22	Co, 8.98

IR (ν, cm^{-1}): 3358 s, 3191 s, 2939 m, 2793 w, 2471 w, 2334 w, 2254 w, 2120 w, 2020 w, 1664 s, 1610 s, 1460 m, 1405 s, 1350 m, 1141 s, 1113 s, 1092 s, 937 w, 891 w, 866 w, 770 w, 627 s, 585 s, 477 m, 456 w.

Powder X-ray diffraction (pXRD) analysis was carried out on a Bruker D8 ADVANCE diffractometer (CuK_α radiation) in the range $2\theta = 5°–80°$ with the step of $2\theta = 0.01125°$ and the exposure at least 0.15 s/step. Diffraction patterns were indexed using the PDF2 database (version 2022).

A set of diffraction reflections for the isolated compounds was collected on a Bruker SMART APEX2 automated diffractometer (MoK_α radiation, graphite monochromator, ω–ϕ scan mode). The data were indexed and integrated using the SAINT program [23]. An absorption correction was applied by measuring equivalent reflections (SADABS) [24]. The structures were solved by a direct method with the subsequent calculation of the difference Fourier syntheses. All non-hydrogen atoms were refined in the anisotropic approximation. All hydrogen atoms of the NH_2 groups, except for the N(1) atom in compound **II**, were refined by the riding model with the thermal parameters $U_{iso} = 1.2U_{eq}$ (U_{iso}) of the corresponding non-hydrogen atom ($1.5U_{iso}$ for CH_3 groups and water molecules).

All calculations were performed using the SHELXTL program [25]. The structures were solved and refined using the OLEX2 software [26]. The main crystallographic data, experimental parameters, and structure refinement characteristics are listed in Table 1.

The crystallographic data were deposited at the Cambridge Crystallographic Data Centre (CIF files CCDC nos. 2300005–2300008 for compounds **II** and **V**–**VII**, respectively).

The thermal behavior of the coordination compounds of cobalt(II) nitrates with carbamide and acetamide was studied using thermogravimetry (TG)–differential scanning calorimetry (DSC) on an SDT Q600 simultaneous thermal analyzer in alundum crucibles. All measurements were carried out in air (100 mL/min) at a linear heating rate of 10°C/min. In the case of the perchlorate samples, the thermal behavior was studied by TG and differential thermal analysis (DTA) in air on a Q-1500 D derivatograph in alundum crucibles at a heating rate of 10°C/min.

The Co_3O_4 samples used for the catalytic studies were prepared by the thermolysis of the isolated complexes in a muffle furnace at 800–900°C in alundum crucibles, and the weight of the formed product was at least 200 mg. The epoxidation of allyl alcohol with hydrogen peroxide was studied at 30°C for 120 min in a closed batch reactor under isothermal conditions with permanent stirring. The composition of the reaction mixture was examined by gas chromatography on a Tsvet gas chromatograph (Russia) using a thermal conductivity detector and a glass packing column (3 m × 3 mm) filled with the 3% OV17 chromatographic phase on chromaton-N-super (helium as the carrier gas (2.1 L/h), isothermal conditions of separation at 160°C, ethyl benzoate as the internal standard). The hydrogen peroxide concentration was determined by iodometric titration. Allyl alcohol (Acros, 99%), a solution of hydrogen peroxide (KHIMMED, 33.7% H_2O_2), glycidol (Acros, 97%), and methanol (99.9%) as the solvent were used. Hydrogen peroxide was introduced into the reactor as a 30% aqueous solution ($c_{AllAl} = 6.00$ mol/L and $c_{HP} = 3.00$ mol/L, where c_{AllAl} and c_{HP} are the concentrations of allyl alcohol and hydrogen peroxide, respectively). The weight of the Co_3O_4 catalyst was 0.0060 g. The experiment with the standard titanosilicate catalyst TS-1 (0.1016 g) for alkene epoxidation was carried out under identical conditions for comparison. The amounts of the catalysts were chosen taking into account the equal metal content in the reaction system. The scheme of the setup is shown in Fig. S1.

RESULTS AND DISCUSSION

Compounds $[Co(Ur)_4](NO_3)_2$ (**I**), $[Co(Ur)_6](NO_3)_2$ (**II**), $[Co(AA)_4(H_2O)_2](NO_3)_2$ (**III**), $[Co(AA)_4(H_2O)_2](NO_3)_2 \cdot 2AA$ (**IV**), $[Co(Ur)_6](ClO_4)_2$ (**V**), $[Co(AA)_4(H_2O)_2](ClO_4)_2$ (**VI**), and $[Co(AA)_6](ClO_4)_2$ (**VII**) were synthesized by the reactions of cobalt

Table 1. Crystallographic data and experimental and refinement data for compounds **II** and **V–VII**

Parameter	Value			
	II	**V**	**VI**	**VII**
Empirical formula	$C_3H_{12}N_7O_6Co_{0.50}$	$C_3H_{12}N_6O_7ClCo_{0.50}$	$C_8H_{24}N_4O_{14}Cl_2Co$	$C_{12}H_{30}N_6O_{14}Cl_2Co$
Crystal sizes, mm	0.22 × 0.18 × 0.11	0.12 × 0.1 × 0.04	0.14 × 0.2 × 0.02	0.2 × 0.2 × 0.01
Crystal color, habitus	Pink, prismatic	Pink, prismatic	Pink, prismatic	Pink, platy
FW	271.66	309.10	530.14	612.25
Crystal system	Monoclinic	Monoclinic	Monoclinic	Triclinic
Space group	$C2/c$	$P2_1/n$	$P2_1/c$	$P\bar{1}$
a, Å	17.012(4)	10.576(12)	6.955(7)	7.753(5)
b, Å	18.057(3)	7.361(5)	16.270(16)	9.521(4)
c, Å	7.3680(9)	14.425(12)	9.737(13)	9.640(5)
α, deg	90	90	90	63.825(13)
β, deg	109.522(7)	102.19(4)	104.31(5)	83.98(2)
γ, deg	90	90	90	83.07(2)
V, Å^3	2133.2(6)	1097.7(17)	1068(2)	632.9(6)
Z	8	4	2	1
μ, mm^{-1}	0.892	1.119	1.125	0.063
ρ_{calc}, g/cm^3	1.692	1.870	1.649	1.606
F(000)	1124	634	546	317
T, K	100	100	100	100
Number of measured/independent reflections	7329/3705	4158/2124	4543/2393	6026/4170
Number of reflections with $I > 2\sigma(I)$	3112	1557	1605	3024
Number of restraints/parameters	0/151	0/160	0/136	0/163
Residual electron density	0.074	0.106	0.109	0.107
Wavelength, Å	0.71073	0.71073	0.71073	0.71073
θ_{min}–θ_{max}, deg	2.256–34.317	2.183–26.008	2.496–27.496	2.358–34.250
Range of indices	$-26 \le h \le 15$, $-27 \le k \le 28$, $-10 \le l \le 11$	$-9 \le h \le 13$, $-8 \le k \le 9$, $-17 \le l \le 15$	$-9 \le h \le 7$, $-20 \le k \le 21$, $-11 \le l \le 12$	$-12 \le h \le 8$, $-14 \le k \le 15$, $-14 \le l \le 15$
GOOF	1.057	1.040	1.027	1.031
R for all reflections/*wR* for reflections with $I \ge 2\sigma(I)$	0.0439/0.0334	0.0995/0.0896	0.1180/0.1036	0.0794/0.0480

nitrate or perchlorate with carbamide or acetamide in various molar ratios.

No reflections of the initial crystalline compounds are observed on the diffraction patterns of the isolated substances (Figs. 1, 2). The experimental diffraction patterns of the isolated complexes and those calculated from the XRD data exhibit good agreement (Figs. 1, 2).

The preliminary conclusion about the character of ligand coordination was drawn on the basis of the IR spectroscopic data (Figs. S2–S8). The absorption bands at 1668 and 1640 cm^{-1}, which are caused by the stretching vibrations of the carbonyl group in the IR spectra of pure acetamide and carbamide, respectively, are shifted to higher wavelengths. This indicates that the ligand is coordinated through the donor oxygen atom [27].

The uncoordinated nitrate ion has four characteristic frequencies: symmetric stretching vibration frequency ν_s(NO) in a range of 1050–1060 cm^{-1}, nonsymmetric doubly degenerate stretching vibration frequency ν_{as}(NO) from 1350 to 1400 cm^{-1}, and two frequencies of bending vibrations $\delta(NO_3^-)$ from 810 to

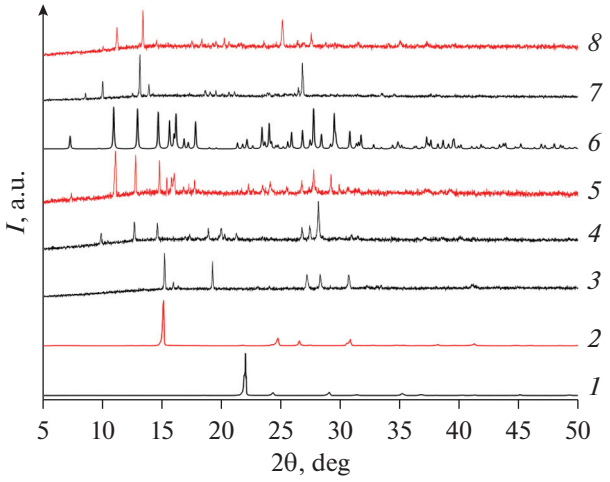

Fig. 1. Powder diffraction patterns of the precursors and isolated nitrate complexes: (*1*) urea, (*2*) acetamide, (*3*) $Co(NO_3)_2 \cdot 6H_2O$, (*4*) **I** (exp.), (*5*) **II** (exp.), (*6*) **II** (calcd.), (*7*) **III** (exp.), and (*8*) **IV** (exp.).

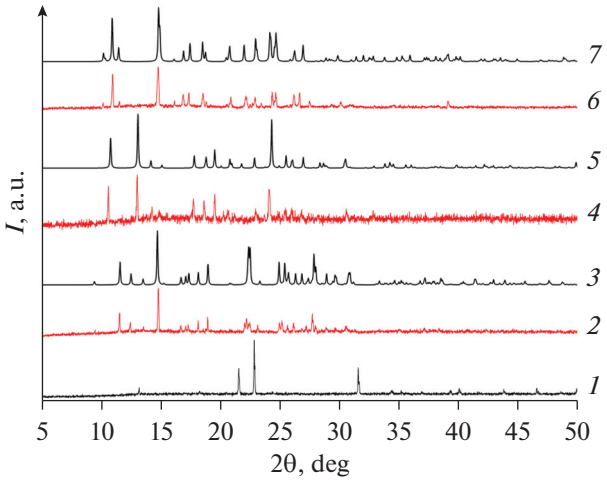

Fig. 2. Powder diffraction patterns of the precursors and isolated perchlorate complexes: (*1*) $Co(ClO_4)_2 \cdot 6H_2O$, (*2*) **V** (exp.), (*3*) **V** (calcd.), (*4*) **VI** (exp.), (*5*) **VI** (calcd.), (*6*) **VII** (exp.), and (*7*) **VII** (calcd.).

840 and from 710 to 730 cm^{-1}. The symmetry decreases upon nitrate ion coordination resulting in the appearance of the following bands in the IR spectrum: the symmetric vibration in the range from 970 to 1040 cm^{-1}, stretching antisymmetric vibration splitted into two high-intensity bands in ranges of 1550–1410 and 1290–1250 cm^{-1}, nonplanar vibration in a range of 830–800 cm^{-1}, and planar bending vibration appeared as two absorption bands in a range of 780–700 cm^{-1} and about 680 cm^{-1}. The spectra of the synthesized nitrate coordination compounds exhibit the absorption bands characteristic of the uncoordinated nitrate ion: 1475 ν(CN), 1384 ν_{as}(inner), 1019 $\nu_s(NO_2)$, 826 $\pi(NO_3)$, and 776 $\delta_{as}(NO_3)$ [28].

The spectra of the perchlorate complexes exhibit bands characteristic of the free perchlorate ion: the symmetric stretching vibration at 936 cm^{-1}, symmetric bending vibration at 460 cm^{-1}, asymmetric stretching vibration at 1110 cm^{-1}, and asymmetric bending vibration at 626 cm^{-1} [28].

The broad bands of stretching vibrations of the O–H and N–H groups in a range of 3500–3300 cm^{-1} indicate the formation of a stable system of hydrogen bonds in the compounds.

The molecular and crystal structures of compounds **I** and **III** were characterized earlier [20–22]. The structures of previously unstudied compounds **II** and **V**–**VII** were determined by XRD.

The crystallographic parameters and experimental details for complexes **II** and **V**–**VII** are given in Table 1.

As shown by the XRD data, the coordination number of the cobalt atom is six in all complexes. In the synthesized complexes, the carbamide and acetamide molecules coordinate via the carbonyl oxygen atom. In the structures of compounds **II**, **V**, and **VII**, the inner sphere contains six molecules of the amide ligand. The structure of complex **VI** contains four acetamide molecules and two water molecules. The nitrate and perchlorate ions in the synthesized compounds are located in the outer sphere and do not coordinate to the cobalt ion, which is consistent with the IR spectroscopic data.

In the structure of complex **II**, the coordination polyhedron is strongly distorted, which is indicated by the O(1)Co(1)O(3) and O(2)Co(1)O(2) angles equal to 173.35° and 174.56°, respectively (Fig. 3). The Co–O–C–N torsion angles have the same sign for equivalent ligands. The characteristics of the bond lengths and bond and torsion angles for complex **II** are given in Table S2.

Different bond lengths indicate different binding strengths of carbamide with the central cobalt(II) ion.

The central cobalt(II) ion in complex **V** also has the coordination environment in the form of a distorted octahedron (Fig. 4). The bond lengths and bond and torsion angles are listed in Table S3.

The presented data show that the distortion of the polyhedron in complex **V** is less pronounced than that in compound **II**.

The coordination polyhedron of complex **VI** is a distorted octahedron formed by the oxygen atoms of the acetamide molecules and water molecules (Fig. 5). The lengths of the bonds of the ligands with the central atom indicate different binding strengths, which are significantly higher for the water molecules. An analysis of the torsion angles shows that the planar geometry of the ligands is insignificantly distorted. The data

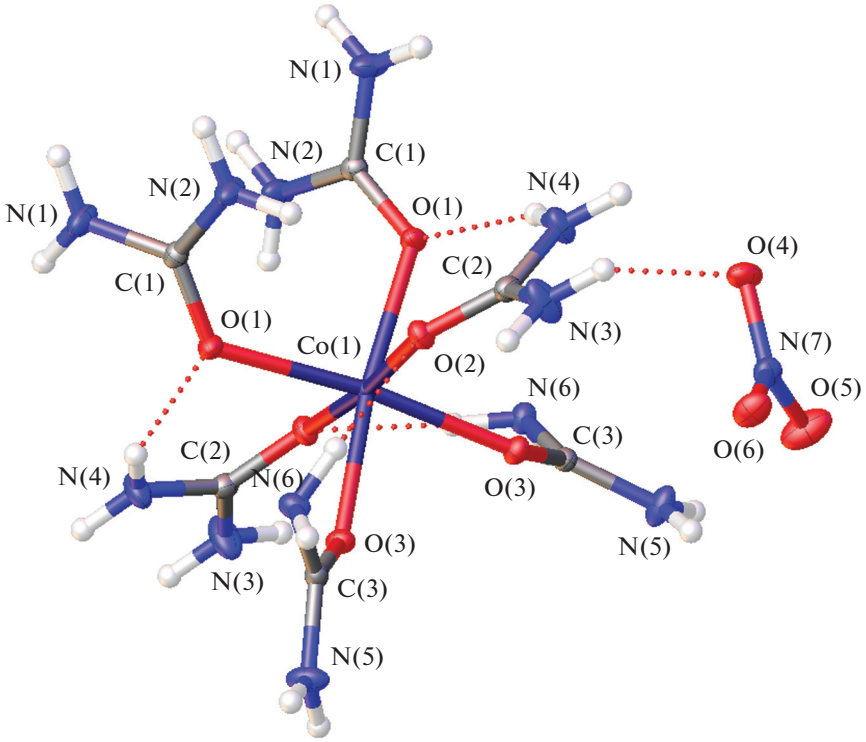

Fig. 3. Fragment of the structure of compound **II**.

on the characteristics of the bond lengths and bond and torsion angles are presented in Table S4.

The coordination polyhedron of complex **VII** (Fig. 6) is an almost regular octahedron: the Co–O bond lengths and bond angles are rather close to each other. The characteristics of the bond lengths and bond and torsion angles are presented in Table S5.

The formation of a system of hydrogen bonds was revealed in all the studied structures, which is consistent with the IR spectroscopic data. The complex cations contain bonds of the N–H...O type between the adjacent molecules of the ligands. The outer-sphere nitrate or perchlorate ions are bound to the coordinated carbamide or acetamide molecules via bonds of the N–H...O type, and bonds of the O–H...O type provide binding with the water molecules (in the structure of complex **VI**). The main characteristics of hydrogen bonds are presented in Tables S6–S9.

Table 2. Results of the thermal decomposition of the nitrate and perchlorate complexes with acetamide and carbamide

Complex	Maxima of endothermic effects, °C	Maxima of exothermic effects, °C	Temperature range of SCS, °C	Temperature of oxide formation, °C
I	78, 145	242, 392	225–423	423
II	130, 228	249, 413	228–440	440
III	102	231, 243	196–293	293
IV	95	217, 257	154–289	289
V	116, 178	325, 341	247–375	375
VI	98	281	263–319	319
VII		283	265–320	320

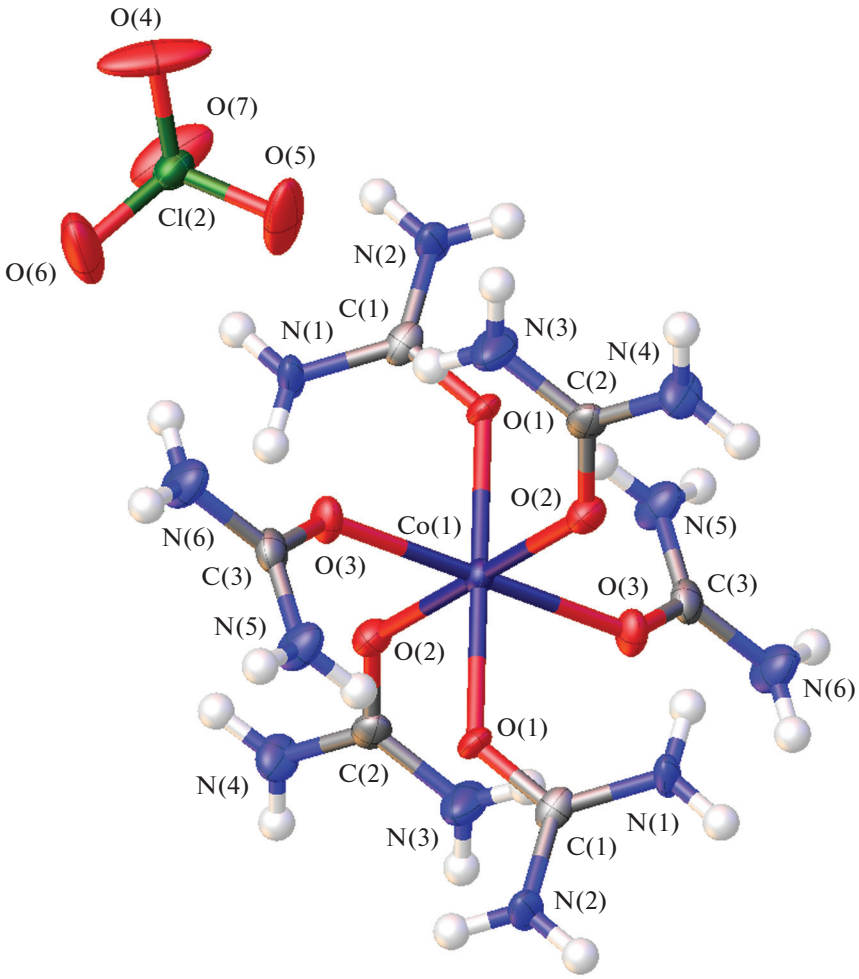

Fig. 4. Fragment of the structure of compound **V**.

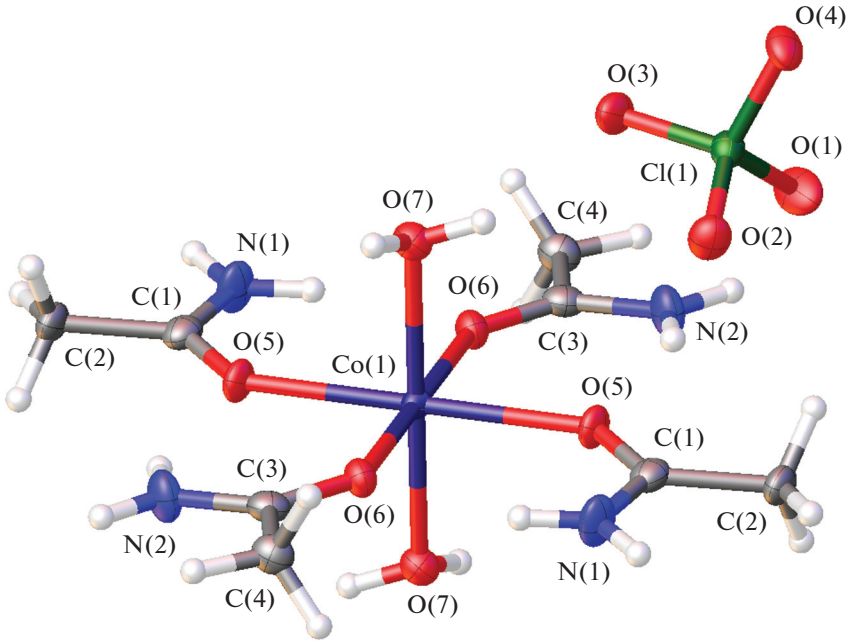

Fig. 5. Fragment of the structure of compound **VI**.

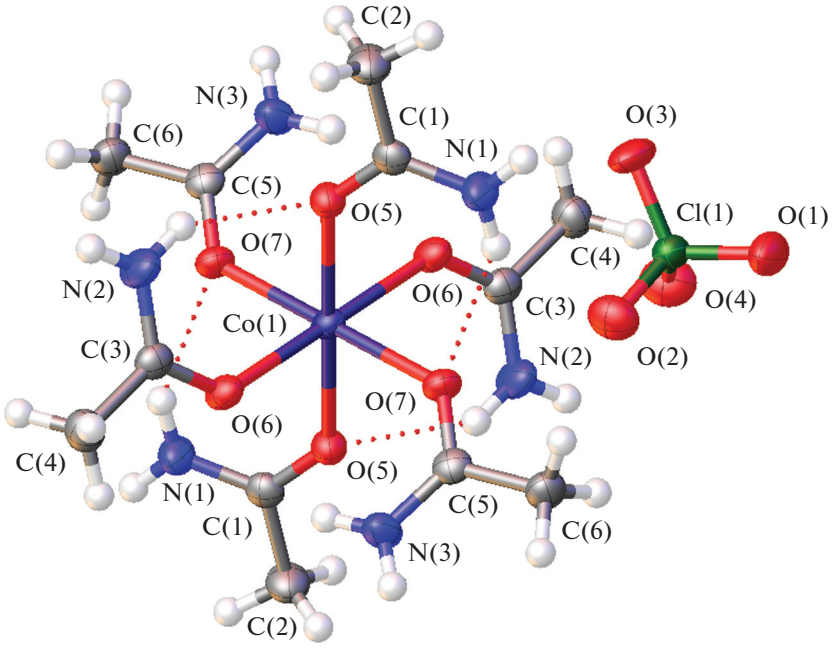

Fig. 6. Fragment of the structure of compound **VII**.

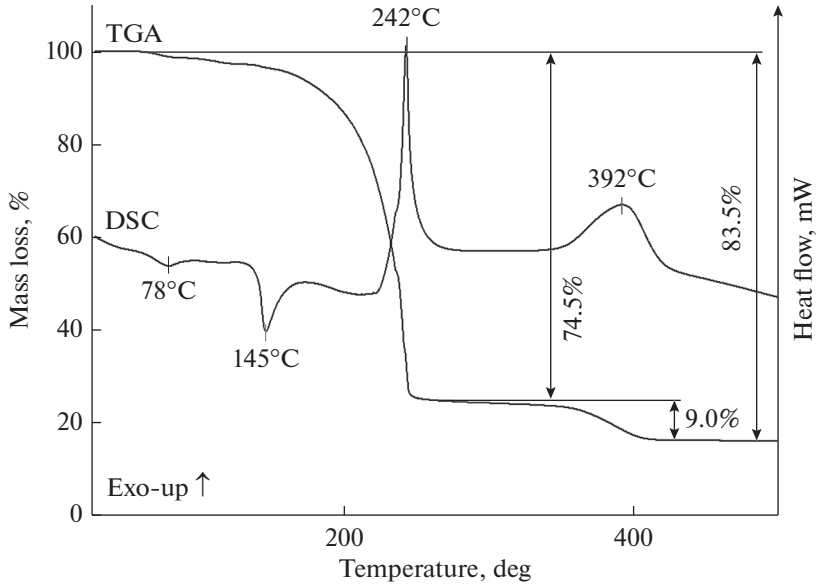

Fig. 7. Thermogram of complex $[Co(Ur)_4](NO_3)_2$ (**I**).

The thermal decomposition of the synthesized compounds modeling the synthesis of cobalt oxide by the SCS method was studied (Table 2).

The thermograms of complexes **I** and **VI** recorded in air are exemplified in Figs. 7 and 8, respectively.

The thermogram of compound **I** exhibits an insignificant endothermic effect with a maximum at 78°C, which can be due to adsorbed water removal, after which melting takes place (maximum at 145°C). A pronounced exothermic effect accompanied by a significant mass loss corresponding to the combustion reaction is observed in a temperature range of 220–280°C (maximum at 242°C). The exothermic effect with a maximum at 392°C corresponds to the oxidation of the remained organic species. The total mass loss at 500°C is about 84%, which corresponds to the

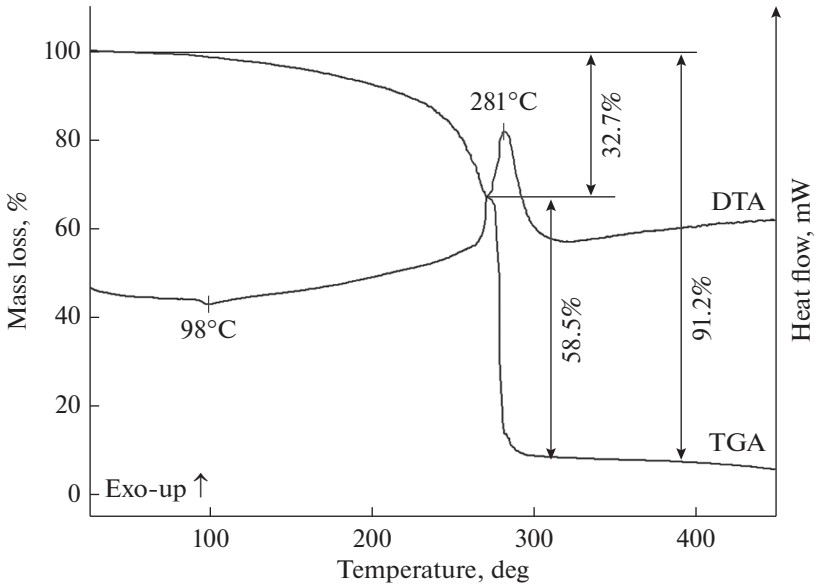

Fig. 8. Thermogram of complex $[Co(AA)_4(H_2O)_2](ClO_4)_2$ (**VI**).

formation of $CoO_{1-\delta}$, the cooling of which in air resulted in the formation of Co_3O_4.

In the case of compound **VI**, melting occurs in a range of 95–103°C. The gradual mass loss in the temperature range to 268°C can be related to the decomposition of some acetamide molecules in the formed melt. A pronounced exothermic effect is observed above 270°C, which is likely a superposition of two effects and caused by the oxidation of the remained AA molecules by the perchlorate ions. The course of the TG and DSC curves above 310°C remains almost unchanged. The decomposition product is also $CoO_{1-\delta}$, which is oxidized to Co_3O_4 on cooling in air.

A possibility of cobalt(II) oxide formation under the studied conditions can be used for the formation of double oxides of the $Co^{II}Fe_2^{III}O_4$ type, which are presently synthesized using other methods [29].

An analysis of the data in Table 2 shows that the temperature of oxide phase formation in the case of acetamide (280–300°C) is considerably lower than that in the case of carbamide (420–440°C). This can be associated with the fact that the heat of combustion of acetamide (1191.5 kJ/mol) is higher than that for carbamide (635.0 kJ/mol).

The thermal decomposition of the perchlorate complexes is accompanied by a decrease in the temperature of oxide phase formation during the thermolysis of the carbamide compounds and by an increase in the temperature in the case of the acetamide complexes as compared to the temperature of decomposition of the nitrate complexes. For instance, for the thermolysis of sample **VI**, the temperature of oxide formation is by 26°C higher than that for compound **III**.

As shown by the pXRD data, the solid residues of all studied complexes at 900°C in air are single-phase samples of Co_3O_4.

The thermal destruction products were analyzed by pXRD (Fig. 9) and transmission electron microscopy (TEM) (Fig. 10). The solid residues of pyrolysis of all isolated complexes at 900°C in air are single-phase samples of Co_3O_4.

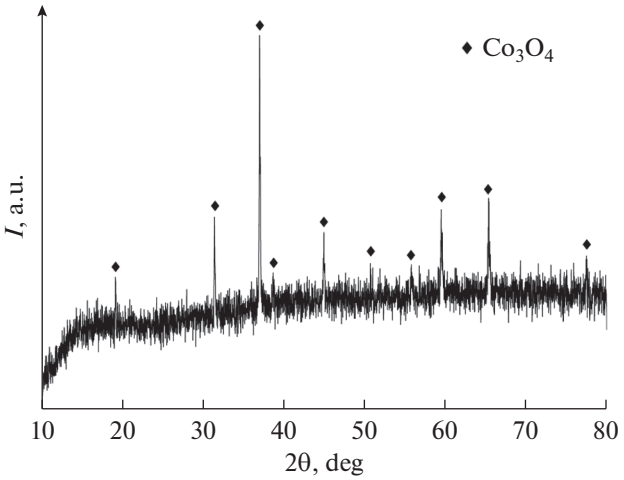

Fig. 9. Powder diffraction pattern of the solid product of the thermolysis of complex **V** (* designate reflections characteristic of Co_3O_4).

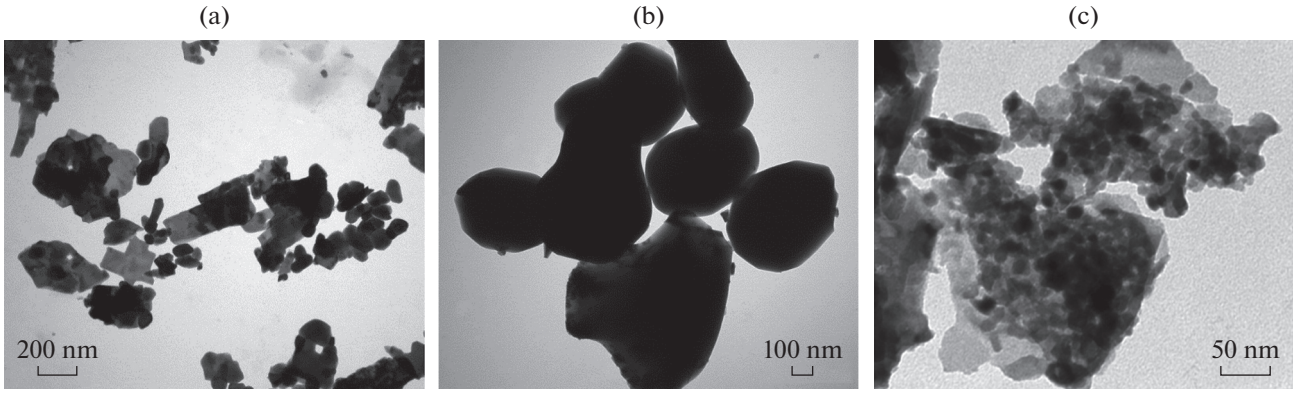

Fig. 10. TEM images of the thermolysis products of compounds (a) **I**, (b) **II**, and (c) **V**.

The particle size distribution was determined from the TEM results (Fig. 11). The values determined by the Debye–Scherrer method (given in parentheses) correlate with the TEM data. The particles 24 (46) nm in size were shown to prevail in the Co_3O_4 sample prepared by the thermolysis of compound **V**. The samples of compounds **I** and **II** are characterized by the particle sizes about 75 (91) and 622 (687) nm, respectively.

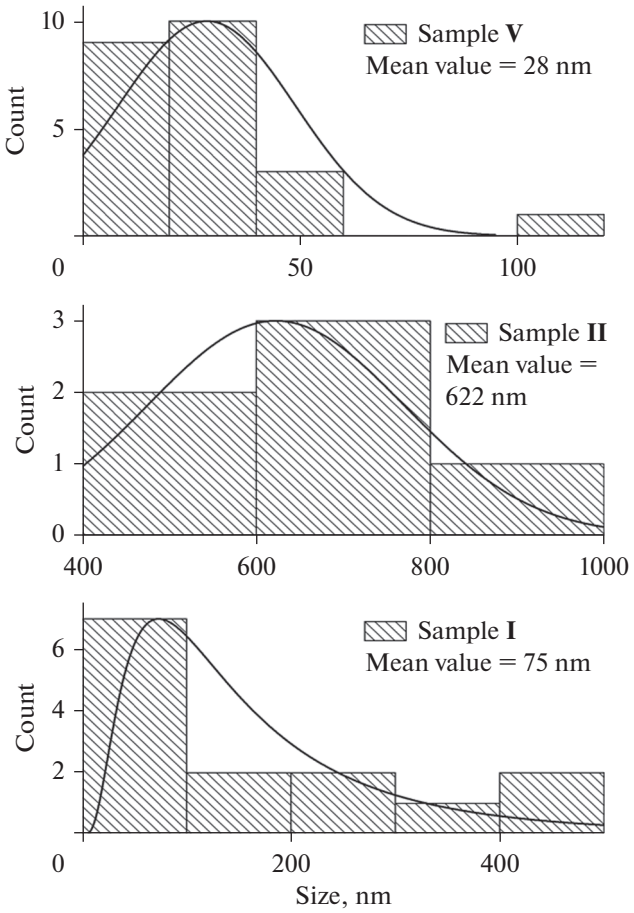

Fig. 11. Particle size distribution of Co_3O_4 prepared by the thermolysis of compounds **I**, **II**, and **V**.

It is known that Co_3O_4 along with such oxides as Fe_3O_4 and Mn_3O_4 is an efficient catalyst in the formation of hydroxyl radicals via the Fenton mechanism in a number of oxidation processes [30]. Therefore, we decided to test the nanosized cobalt oxide prepared by the above described method as the catalyst in the epoxidation of allyl alcohol to glycidol.

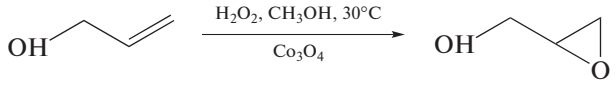

The catalytic activities of the cobalt oxide prepared in this work and the industrial catalyst (titanium-containing zeolite TS-1 [31]) are compared in Table 3.

An advantage of the formed Co_3O_4 is a high selectivity of product formation to hydrogen peroxide comparable with the same parameter for the industrial catalyst. Oxide Co_3O_4 also provided the allyl alcohol formation comparable with the conversion of the substrate under the catalytic conditions using TS-1. The low selectivity of formation of the product to allyl alcohol is likely due to the formation of large amounts of oligomers from glycidol deactivating the catalyst and retarding the process. Therefore, the process almost ceases in 15 min. The nanosized cobalt oxide is inferior to the TS-1 catalyst of the low-temperature epoxidation of alkenes but can be recommended for studying the catalytic activity in other processes using hydrogen peroxide.

To conclude, the reactions of cobalt(II) nitrate or perchlorate with acetamide or carbamide afford the following complexes: $[Co(Ur)_4](NO_3)_2$, $[Co(Ur)_6](NO_3)_2$, $[Co(AA)_4(H_2O)_2](NO_3)_2$, $[Co(AA)_4(H_2O)_2](NO_3)_2{\cdot}2AA$, $[Co(Ur)](ClO_4)_2$, $[Co(Ur)_6](ClO_4)_2$, $[Co(AA)_4(H_2O)_2](ClO_4)_2$, and $[Co(Ur)_6](ClO_4)_2$. These complexes are intermediates in the

Table 3. Selected technological parameters of the catalytic reaction

Catalyst	Co_3O_4	TS-1
Conversion of allyl alcohol, %	21.5	26.0
Selectivity of formation of glycidol to allyl alcohol, %	6.0	83.8
Conversion of hydrogen peroxide, %	2.5	44.6
Selectivity of formation of glycidol to hydrogen peroxide, %	93.8	99.8

preparation of cobalt oxide by the self-propagating high-temperature synthesis.

The thermal decomposition of the synthesized complexes affords oxide Co_3O_4, whose particle size varies from 75 to 650 nm.

SUPPLEMENTARY INFORMATION

The online version contains supplementary material available at https://doi.org/10.1134/S1070328424600049.

ACKNOWLEDGMENTS

Elemental analysis was conducted at the Center for Collective Use of the MIREA Russian Technological University and supported by the Ministry of Science and Higher Education of the Russian Federation. Powder X-ray and single-crystal diffraction analyses were carried out at the Center for Collective Use of Physical Methods of Investigation at the Kurnakov Institute of General and Inorganic Chemistry of the Russian Academy of Sciences. Thermal analysis was conducted using the equipment of the Center for Facility Collection at the National Research Center Kurchatov Institute.

FUNDING

This study was supported by the Russian Science Foundation, project no. 21-19-00403.

CONFLICT OF INTEREST

The authors of this work declare that they have no conflicts of interest.

REFERENCES

1. Vereshchagin, A.L. *Preparativnyi samorasprostranyayushchiisya vysokotemperaturnyi sintez oksidov* (Preparative Self-Propagating High-Temperature Synthesis of Oxides), Biisk, 2013.
2. Merzhanov, A.G., *Izv. Vysshikh. Uchebn. Zaved.*, 2006, no. 5, p. 5.
3. Din, A., Akhtar, K., Karimov, Kh.S., et al., *J. Mol. Liq.*, 2017, vol. 237, p. 266.
4. Deng, J., Kang, L., Bai, G., et al., *Electrochim. Acta*, 2014, vol. 132, p. 127.
5. Petrichko, M.I., Karavaev, I.A., Savinkina, E.V., et al., *Russ. J. Inorg. Chem.*, 2023, vol. 68, no. 4, p. 415. https://doi.org/10.1134/S0036023623600193
6. Zhuravlev, V.D., Bamburov, V.G., Beketov, A.R., et al., *Ceram. Int.*, 2013, vol. 39, no. 2, p. 1379.
7. Savinkina, E.V., Karavaev, I.A., Grigoriev, M.S., et al., *Inorg. Chim. Acta*, 2022, vol. 532, p. 120759.
8. Podbolotov, K.B., Volochko, A.T., and Khort, A.A., *Perspektivnye materialy i tekhnologii* (Prospective Materials and Technologies), Klubovich, V.V., Ed., Vitebsk: UO VGTU, 2017, vol. 2, p. 171.
9. Wen, W., Wu, J.-M., and Tu, J.-P., *J. Alloys Comp.*, 2012, vol. 513, p. 592.
10. Jung, J.C.Y., Sui, P.C., and Zhang, J., *J. Energy Storage*, 2021, vol. 35, p. 102217.
11. Hu, X., Wei, L., Chen, R., et al., *ChemSelect*, 2020, vol. 5, no. 17, p. 5268.
12. Vojisavljevic, K., Wicker, S., Can, I., et al., *Adv. Powder Technol.*, 2017, vol. 28, no. 4, p. 1118.
13. Ma, J., Wei, H., Liu, Y., et al., *Int. J. Hydrogen Energy*, 2020, vol. 45, p. 21205.
14. Toniolo, J.C., Takimi, A.S., and Bergmann, C.P., *Mater. Res. Bull.*, 2010, vol. 45, no. 6, p. 672.
15. Groven, L.J., Pfeil, T.L., and Pourpoint, T.L., *Int. J. Hydrogen Energy*, 2013, vol. 38, no. 15, p. 6377.
16. Luo, J. and Yathirajan, H.S., *Ind. J. Mater. Sci.*, 2013, vol. 2014, p. 787306.
17. Rau, T.F. and Kurkutova, E.N., *Dokl. Akad. Nauk SSSR*, 1971, vol. 204, no. 2, p. 342.
18. Krawchuk, A. and Stadnicka, K., *Acta Crystallogr., Sect. C: Cryst. Chem. Commun.*, 2007, vol. 63, p. 448.
19. Rau, T.F. and Kurkutova, E.N., *Dokl. Akad. Nauk SSSR*, 1972, vol. 204, no. 3, p. 600.
20. Gentile, P.S., White, J., and Haddad, S., *Inorg. Chim. Acta*, 1974, vol. 8, p. 97.
21. Gentile, P.S., Carfagno, P., Haddad, S., et al., *Inorg. Chim. Acta*, 1972, vol. 6, p. 296.
22. McGillicuddy, R.D., Thapa, S., Wenny, M.B., et al., *J. Am. Chem. Soc.*, 2020, vol. 142, no. 45, p. 19170.
23. *SAINT*, Madison: Bruker AXS Inc., 2018.
24. Krause, L., Herbst-Irmer, R., Sheldrick, G.M., and Stalke, D., *J. Appl. Crystallogr.*, 2015, vol. 48, no. 1, p. 3.
25. Sheldrick, G.M., *Acta Crystallogr., Sect. C: Struct. Chem.*, 2015, vol. 71, p. 3.

26. Dolomanov, O.V., Bourhis, L.J., Gildea, R.J., et al., *J. Appl. Crystallogr.*, 2009, vol. 42, p. 339.

27. Nakamoto, K., *Infrared Spectra and Raman Spectra of Inorganic and Coordination Compounds*, New York: Wiley, 1986.

28. Rosenthal, M.R., *J. Chem. Educ.*, 1973, vol. 50, no. 5, p. 331.

29. Nikishina, E.E., *Tonkie Khim. Tekhnol.*, 2021, vol. 16, no. 6, p. 502.

30. Shokri, A. and Fard, M.S., *Environmental Challenges*, 2022, vol. 7, p. 100534.

31. Pastukhova, Zh.Yu., Levitin, V.V., Katsman, E.A., and Bruk, L.G., *Kinet. Katal.*, 2021, vol. 62, no. 5, p. 551.

Translated by E. Yablonskaya